



## ORIGINAL ARTICLE

# Chemical and biological analysis of 4-acyloxy-3-nitrocoumarins as trypanocidal agents



Francisco Salgado<sup>a,b</sup>, Mauricio Moncada-Basualto<sup>a,c</sup>, Josue Pozo-Martinez<sup>a,c</sup>, Ana Liempi<sup>c</sup>, Ulrike Kemmerling<sup>c</sup>, Juan-Diego Maya<sup>b</sup>, Pablo Jaque<sup>d</sup>, Fernanda Borges<sup>e</sup>, Eugenio Uriarte<sup>f</sup>, Maria J. Matos<sup>e,f,\*</sup>, Claudio Olea-Azar<sup>a,\*</sup>

<sup>a</sup> Laboratory of Free Radicals and Antioxidants, Faculty of Chemical and Pharmaceutical Sciences, University of Chile, Sergio Livingstone Polhammer 1007, Independencia, Santiago, Chile

<sup>b</sup> Department of Molecular Pharmacology and Clinical, Faculty of Medicine, University of Chile, Santiago, Chile

<sup>c</sup> Programa Disciplinario de Anatomía y Biología del Desarrollo, Faculty of Medicine, University of Chile, Santiago, Chile

<sup>d</sup> Department of Organic & Físicoquímica, University of Chile, Sergio Livingstone Polhammer, 1007 Independencia, Santiago, Chile

<sup>e</sup> CIQUP/Department of Chemistry and Biochemistry, Faculty of Sciences, University of Porto, Rua Campo Alegre 687, 4169-007 Porto, Portugal

<sup>f</sup> Department of Organic Chemistry, Faculty of Pharmacy, University of Santiago de Compostela, Santiago de Compostela, Spain

Received 8 October 2020; accepted 27 December 2020

Available online 5 January 2021

## KEYWORDS

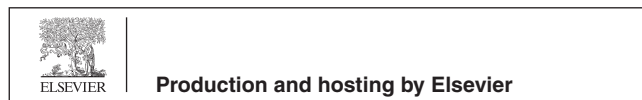
Nitrocoumarins;  
*Trypanosoma cruzi*;  
ROS;  
Fukui index

**Abstract** Chagas disease is the most widespread contagious tropical disease in Latin America, being an important public health problem. Treatments against this disease are still very ineffective, presenting several side effects. Therefore, the search for alternative therapeutic solutions is urgent. In the present work, we evaluate the trypanocidal activity and the mechanism of action of a select series of synthetic 4-acyloxy-3-nitrocoumarins. All the coumarin derivatives showed moderate trypanocidal activity in trypomastigotes, along with low cytotoxicity. In addition, compound **1** decreased the number of infected Vero cells in an intracellular *T. cruzi* model. Electron spin resonance and electrochemical studies showed the formation of nitro radical anions. The Fukui index provided additional information to elucidate the proposed reduction mechanism. Furthermore, *in vitro* radical formation studies demonstrated the potential of these compounds to achieve higher concentrations of intracellular free radicals, proposing oxidative stress as a possible trypanocidal mechanism. Furthermore, no correlation was observed between the diffusion of these compounds,

\* Corresponding author.

E-mail addresses: mariajoao.correiapinto@usc.es, maria.matos@fc.up.pt (M.J. Matos), colea@uchile.cl (C. Olea-Azar).

Peer review under responsibility of King Saud University.



which shows that lipophilicity is not a predominant factor for activity. Elsevier Ltd. All rights reserved.

© 2020 The Author(s). Published by Elsevier B.V. on behalf of King Saud University. This is an open access article under the CC BY-NC-ND license (<http://creativecommons.org/licenses/by-nc-nd/4.0/>).

## 1. Introduction

American trypanosomiasis or Chagas disease, is a life-threatening disease caused by the infection of the protozoan parasite *Trypanosoma cruzi* (*T. cruzi*) (Lazarin-Bidóia et al., 2013; Pérez-Molina & Molina, 2018). In Latin America, Chagas disease is a major public health issue, being amongst the vector-borne diseases with the highest prevalence and mortality, followed by Malaria (Bonney, 2014; Malik, Singh, & Amsterdam, 2015).

During *T. cruzi* life cycle, different morphological stages are observed, which are characterized by relative positions of flagellum, kinetoplast and nucleus (Irigoin et al., 2008). The biological cycle begins when insects (*Triatoma infestans*) become contaminated by consuming blood of mammals presenting the parasite (blood trypomastigotes). In the upper digestive tract, parasites differentiate into the epimastigote form. After advancing to the lower intestine, the parasites covert into the metacyclic trypomastigote form in the vicinity of the rectum. Finally, when the insect defecates near the area where it feeds, parasites enter the bloodstream and infect macrophages and any nucleated cell, ultimately differentiating in the intracellular replicative form known as amastigote (Rassi, Rassi, & Marcondes de Rezende, 2012; Souza, 2005; Teixeira, Hecht, Guimaro, Sousa, & Nitz, 2011; Zingales et al., 2012).

Currently, drugs used to treat this disease are nifurtimox (NFX) and benznidazole (BNZ). Both have been mainstay of parasitocidal treatment for almost 50 years. Even if they are effective for acute infections, their use in chronic patients remains controversial since both drugs show severe side effects (Estani et al., 1998; Fernández et al., 2016). Therefore, it is necessary and urgent the development of new, more effective and less toxic drugs.

It has been described that one of the possible mechanisms of action for NFX would be through the formation of reactive oxygen species (ROS) and/or electrophilic metabolites (Maya et al., 2007; Wilkinson, Taylor, Horn, Kelly, & Cheeseman, 2008). An increase of these species would cause cellular damage and induce apoptotic processes, interfering with mitochondrial functions, thus affecting cell bioenergetics. (Boiani et al., 2010; Maya et al., 2007; Claudio Olea-Azar et al., 2003; Paiva, Medei, & Bozza, 2018). In this context, there is evidence of coumarins that have increased ROS generation as well as mitochondrial function (Aguilera-Venegas, Olea-Azar, Arán, & Speisky, 2013; Robledo-O’Ryan et al., 2017; Rodríguez-Hernández, Martínez, Reyes-Chilpa, & Espinoza, 2020).

Coumarins are a chemical family of high interest in Medicinal Chemistry, given the broad spectrum of pharmacological activities they may display (Borges, Roleira, Milhazes, Santana, & Uriarte, 2005; Iaroshenko et al., 2011; Maria Joao Matos et al., 2009; Riveiro et al., 2010), such as: neuroprotective (Maria João Matos et al., 2015; 2014; 2010) (Jameel, Umar, Kumar, & Hoda, 2016), anti-inflammatory (Hadjipavlou-Litina, Litinas, & Kontogiorgis, 2008), antioxi-

dant (Maria João Matos et al., 2013; F. Pérez-Cruz et al., 2012; K. Pérez-Cruz et al., 2018; Vazquez-Rodriguez et al., 2013) and antihypertensive (Razavi, Arasteh, Imenshahidi, & Iranshahi, 2015), among others. Likewise, coumarins with trypanocidal activity have been described, whose potency depends on the substituents linked to the main scaffold. The trypanocidal mechanism of action of this family of compounds has not been fully elucidated and seems to depend on the substitution patterns. It may be related to the generation of oxidative stress, mitochondrial function, inhibition of essential enzymes for the parasite survival, among others (Figueroa-Guinez et al., 2015; Govêa et al., 2020; Guíñez et al., 2013; Ribeiro et al., 2020; Rodríguez-Hernández et al., 2019; Santos, de Araújo, Giarolla, Seoud, & Ferreira, 2020; Soares et al., 2019; Uliassi et al., 2017).

Our research group previously studied a series of hydroxy 3-arylcoumarins. Trypanocidal activity was evaluated on both epimastigote and trypomastigote forms. These studies demonstrated moderate trypanocidal activity, which was associated with the generation of oxidative stress in the parasite. This mechanism of action was determined through electronic spin resonance (ESR) studies using the spin trapping technique, observing the formation of hydroxyl radicals, carbon centered radicals and DMPOX (using DMPO as a spin trap) (Robledo-O’Ryan et al., 2017).

Based on the above, we also synthesized a series of new 3-carboxamidocoumarins, using different electron acceptors and donors linked to aromatic group, and evaluated the trypanocidal activity both in the infective form of parasite and epimastigotes. The most active compounds from that series contain nitro groups and quinoline substituents. The last ones presented similar IC<sub>50</sub> to NFX on the epimastigote form. Compounds with nitro groups presented high cytotoxicity against mammalian cells unlike those with quinolines. Regarding the mechanism of action, we reported variations in the mitochondrial membrane potential, which were directly related to the dysfunction of this organelle (Muñoz et al., 2016).

Finally, we also evaluated the trypanocidal activity of a 3-amidocoumarins. In this series, the presence of an electron donor at position 4 of the coumarin scaffold and different substituents linked to the amide group, were evaluated. The presence of a hydroxyl group at position 4 was found to decrease the trypanocidal activity in the infective form of *T. cruzi*. The proposed mechanism of action was the generation of oxidative stress, which was directly correlated with the absence of hydroxyl groups in those compounds, that produced the greatest number of free radicals in the parasite. Therefore, it is interesting to evaluate coumarins with electron acceptor groups that have been described as free radical generators (Moncada-Basualto et al., 2018).

Based on the previously described background, in this work the trypanocidal activity of a series of new coumarins containing nitro groups at position 3 was synthesized and evaluated. Groups of different chemical nature at position 4 were

included to understand their role both in intracellular trypanocidal activity as well as bioavailability.

## 2. Experimental section

### 2.1. Chemistry

#### 2.1.1. General information

All reagents were purchased from Sigma-Aldrich and used without further purification. All solvents were commercially available grade. All reactions were carried out under argon atmosphere, unless otherwise mentioned. Reaction mixtures were purified by flash column chromatography using Silica Gel high purity grade (Merck grade 9385 pore size 60 Å, 230–400 mesh particle size). Reaction mixtures were analyzed by analytical thin-layer chromatography (TLC) using plates precoated with silica gel (Merck 60 F254, 0.25 mm). Visualization was accomplished with UV light (254 nm) or potassium permanganate (KMnO<sub>4</sub>). <sup>1</sup>H NMR and <sup>13</sup>C NMR spectra were recorded on a Bruker AMX spectrometer at 250 and 75.47 MHz in the stated solvents (CDCl<sub>3</sub> or DMSO-*d*<sub>6</sub>) using tetramethylsilane (TMS) as an internal standard. Chemical shifts were reported in parts per million (ppm) on the δ scale from an internal standard (NMR descriptions: s, singlet; dd, double-doublet; t, triplet; td, triple-doublet; m, multiplet). Mass spectroscopy was performed using a Hewlett-Packard 5988A spectrometer. This system is an automated service utilizing electrospray (ESI) ionization. Elemental analyses were performed using a Perkin-Elmer 240B microanalyser and were within (0.4% of calculated values in all cases. The purity of compounds was assessed by HPLC and was found to be higher than 98%.

#### 2.1.2. Synthetic methodology

In a round bottom flask, 50 mg of the 4-hydroxy-3-nitrocoumarin are dissolved in 3 mL of DCM. Afterwards, 21 μL of pyridine is added to the mixture, and the mixture is cooled to 0 °C. To this mixture, in the cold, 47 mg of the corresponding acid chloride are added little by little, and the reaction is left stirring overnight, at room temperature. The product obtained is evaporated in vacuo and purified by chromatographic column (hexane/ethyl acetate 1:1).

**3-nitrocoumarin-4-yl-nicotinate (1).** Yield: 53%. <sup>1</sup>H NMR (DMSO-*d*<sub>6</sub>) δ: 7.13–7.22 (m, 1H, H-5'), 7.46–7.53 (m, 1H, H-7), 7.84–7.87 (m, 2H, H-6, H-8), 8.06–8.11 (m, 1H, H-5), 8.59–8.67 (m, 1H, H-6'), 8.92–8.97 (m, 1H, H-4'), 9.17 (s, 1H, H-2'). <sup>13</sup>C NMR (DMSO-*d*<sub>6</sub>) δ: 116.3, 117.5, 124.4, 125.8, 126.0, 126.1, 127.5, 128.7, 132.4, 142.0, 146.3, 146.4, 148.8, 148.9, 164.9. ESI-MS *m/z* (%): 312 (M<sup>+</sup>, 83). Ana. Elem. Calc. for C<sub>15</sub>H<sub>8</sub>N<sub>2</sub>O<sub>6</sub>: C, 57.70; H, 2.58. Found: C, 57.66; H, 2.57.

**3-nitrocoumarin-4-yl-furan-2-carboxylate (2).** Yield: 59%. <sup>1</sup>H NMR (DMSO-*d*<sub>6</sub>) δ: 7.13–7.22 (m, 1H, H-4'), 7.46–7.53 (m, 1H, H-6), 7.86 (dd, 1H, H-8, *J* = 7.8, 1.6), 8.02–8.08 (m, 2H, H-7, H-5'), 8.59 (dd, 1H, H-5, *J* = 7.8, 1.6), 8.88–8.91 (m, 1H, H-3'). <sup>13</sup>C NMR (DMSO-*d*<sub>6</sub>) δ: 111.2, 116.4, 116.7, 121.5, 124.0, 125.8, 127.3, 133.3, 141.6, 146.5, 150.1, 152.3, 156.4, 164.0. ESI-MS *m/z* (%): 301 (M<sup>+</sup>, 91). Ana. Elem. Calc. for C<sub>14</sub>H<sub>7</sub>NO<sub>7</sub>: C, 55.83; H, 2.34. Found: C, 55.80; H, 2.37.

**3-nitrocoumarin-4-yl-dimethylcarbamate (3).** Yield: 64%. <sup>1</sup>H NMR (DMSO-*d*<sub>6</sub>) δ: 2.49 (s, 6H, 2xCH<sub>3</sub>), 7.17 (dd, 1H, H-8,

*J* = 7.7, 1.6), 7.46–7.53 (m, 1H, H-6), 7.84–7.88 (m, 1H, H-7), 8.05 (dd, 1H, H-5, *J* = 7.7, 1.6). <sup>13</sup>C NMR (DMSO-*d*<sub>6</sub>) δ: 39.7, 116.8, 117.3, 123.1, 125.1, 128.0, 129.7, 150.9, 155.8, 156.5, 164.2. ESI-MS *m/z* (%): 278 (M<sup>+</sup>, 91). Ana. Elem. Calc. for C<sub>12</sub>H<sub>10</sub>N<sub>2</sub>O<sub>6</sub>: C, 51.81; H, 3.62. Found: C, 51.85; H, 3.60.

**3-nitrocoumarin-4-yl-thiophene-2-carboxylate (4).** Yield: 56%. <sup>1</sup>H NMR (DMSO-*d*<sub>6</sub>) δ: 7.19 (t, 1H, H-4', *J* = 6.7), 7.50 (td, 1H, H-6, *J* = 7.7, 1.5), 7.87 (dd, 1H, H-8, *J* = 7.7, 1.5), 8.06 (t, 1H, H-3', *J* = 6.7), 8.55 (td, 1H, H-7, *J* = 7.7, 1.5), 8.90–8.95 (m, 2H, H-5, H-5'). <sup>13</sup>C NMR (DMSO-*d*<sub>6</sub>) δ: 116.7, 117.6, 123.7, 126.3, 127.6, 128.1, 128.9, 129.3, 132.9, 134.2, 143.6, 146.0, 153.1, 160.3. ESI-MS *m/z* (%): 317 (M<sup>+</sup>, 90). Ana. Elem. Calc. for C<sub>14</sub>H<sub>7</sub>NO<sub>6</sub>S: C, 53.00; H, 2.22. Found: C, 52.98; H, 2.25.

**3-nitrocoumarin-4-yl-benzoate (5).** Yield: 71%. <sup>1</sup>H NMR (DMSO-*d*<sub>6</sub>) δ: 7.14–7.22 (m, 1H, H-8), 7.46–7.63 (m, 4H, H-6, H-7, H-3', H-5'), 7.85–7.94 (m, 2H, H-2', H-6'), 8.06–8.12 (m, 1H, H-4'), 8.92–8.95 (m, 1H, H-5). <sup>13</sup>C NMR (DMSO-*d*<sub>6</sub>) δ: 116.1, 123.0, 125.6, 127.3, 128.6, 129.2, 130.7, 132.2, 132.9, 141.9, 146.5, 152.4, 167.4. ESI-MS *m/z* (%): 311 (M<sup>+</sup>, 85). Ana. Elem. Calc. for C<sub>16</sub>H<sub>9</sub>NO<sub>6</sub>: C, 61.74; H, 2.91. Found: C, 61.77; H, 2.93.

### 2.2. Electrochemical studies

#### 2.2.1. Cyclic voltametric

Electrochemical characterization of the new compounds was performed through cyclic voltametric (CV) on a 693 VA Metrohm instrument equipped with a 694 VA Stand converter and 693 VA processor. Potentials were recorded against the Ag/AgCl reference electrode, a hanging drop of mercury (HMDE) was used as a working electrode and platinum as an auxiliary electrode. Tetrabutylammonium perchlorate (TBAP, 0.1 M) in DMSO was used as a supporting electrolyte under an N<sub>2</sub> atmosphere at room temperature. Potential sweeps were executed between –0.6 and –1.8 V, and 0.1–2.5 V/s.

#### 2.2.2. Monitoring of electrochemically generated radicals by ESR

ESR spectra were recorded in the X band (9.85 GHz) using a Bruker ECS106 spectrometer with a rectangular cavity and 50-kHz field modulation. The hyperfine splitting constants were estimated to be accurate within 0.05 G. Nitrocoumarin radicals were generated by an *in situ* electrolytic reduction process under the same experimental conditions as those of CV, in DMSO, with 0.1 M of TBAP. The reduction potentials were acquired from CV. Every spectrum was obtained after 50 scans. ESR spectra were simulated using the program EPR-WinSIM Version 0.98 (Davies, 2016; Duling, 1994).

### 2.3. Computational details

Full geometry optimizations for the 4-acyloxy-3-nitrocoumarins in their neutral states were performed at the dispersion-corrected B3LYP level of theory (B3LYP-D3) combined with the Def2SVP basis set. Harmonic vibrational frequencies were also performed to confirm optimized structures on potential energy surfaces as minima. Fukui indices for nucleophilic attack for every atomic *k* site, *f<sub>k</sub><sup>+</sup>*, (Yang & Mortier, 1986) were calculated using natural atomic

charges,  $q_k$ , (Reed, Weinstock, & Weinhold, 1985) in both neutral ( $N$ ) and anionic ( $N + 1$ ) states at the B3LYP-D3/Def2TZVP//Def2SVP level of theory, for the purpose to gain understanding the reduction process associated with the anion radical formation. This index was computed as stated Eq. (1).

$$f_k^+ = q_k(N) - q_k(N + 1) \quad (1)$$

All calculations were performed using Gaussian09 suite of programs (Frisch et al. (2009)).

## 2.4. Biological studies

### 2.4.1. Cytotoxicity assay

The effect of the new coumarins on RAW 264.7 cells was evaluated through the tetrazolium dye (MTT; 3-(4,5-dimethylthiazol-2-yl)-2,5-di-phenyltetrazolium bromide) assay, as a viability test (Mosmann, 1983). Briefly, 10  $\mu$ L of 5 mg/mL MTT plus 0.22 mg/mL phenazine methosulfate (electron carrier) (Bisby, Brooke, & Navaratnam, 2008), were added to each well containing RAW 264.7 cell culture, in 100  $\mu$ L RPMI 1640 without phenol red. Compounds under study, dissolved in DMSO, were added to the culture media at the concentrations demonstrated in the figures and tables. DMSO final concentration was less than 0.25% v/v. After incubation for 4 h at 37 °C, the generated water-insoluble formazan dye was dissolved by the addition of 100  $\mu$ L of 10% w/v sodium dodecyl sulphate (SDS) in 0.01 M HCl. The plates were further incubated overnight at 37 °C, and optical density of the wells was determined using a micro-plate reader (Asys Expert Plus®, Asys Hitach, Austria) at 570 nm. Under these conditions, the optical density is directly proportional to the viable cell number in each well. All the experiments were performed at least three times and data reported as means and their standard deviations from triplicate cultures. Results are reported as the percentage of non-viable RAW 264.7 cells regarding the control.

### 2.4.2. Determination of the activity in trypomastigotes, viability study

Primary cultures of peritoneal macrophage from chagasic mice were used as the source of *T. cruzi* trypomastigotes. Vero cells were cultured in 5% fetal bovine serum supplemented RPMI 1640 medium in humidified air with 5% CO<sub>2</sub> at 37 °C. Then, cells were infected with the trypomastigotes at a multiplicity of infection (MOI) of 3. After incubation at 37 °C in humidified air and 5% CO<sub>2</sub>, for 5–7 days the culture medium was centrifuged at 500g for 5 min. The trypomastigote containing pellet was re-suspended in free-serum RPMI 1640 and penicillin–streptomycin at a final density of 1x10<sup>7</sup> parasites/mL. The trypomastigote viability was determined by the previously described MTT assay incubating 1x10<sup>7</sup> parasites/mL in free-serum RPMI 1640 culture medium at 37 °C during 24 h with or without the studied compounds. Untreated parasites were used as controls (100% of viability). Compound was evaluated at different concentrations (10–250  $\mu$ M) to determinate the IC<sub>50</sub> values.

### 2.4.3. Detection of radical species in parasite by ESR

*T. cruzi* epimastigotes (Dm28c), from our collection (Programa de Farmacología Molecular y Clínica, Facultad de Medicina, Universidad de Chile, Santiago, Chile), were maintained in liver infusion tryptose (LIT) medium supplemented

with 10% heat-inactivated FBS at 28 °C. Parasites were harvested by 500 g centrifugation for 10 min. The pellet was suspended in PBS to archive a final suspension of 8x10<sup>7</sup> parasites/mL. A suspension of 8x10<sup>7</sup> epimastigotes correspond to 1 mg protein or 12 mg of fresh weight. ESR spectra were obtained using epimastigotes, in a reaction medium containing 1 mM NADPH and 100 mM DMPO, in 20 mM phosphate buffer, pH 7.4. All experiments were done after of 10 min of incubation, at 28 °C, for each 3-nitrocoumarins (5 mM) with epimastigotes of *T. cruzi* (1 mg/100  $\mu$ L), NADPH and DMPO, in an aerobic environment.

### 2.4.4. Generation of ROS in *T. cruzi* cultures

For the detection of ROS, 2',7'-dichlorodihydrofluorescein diacetate (DCFH<sub>2</sub>-DA) method was used. 96-well plates were seeded with 1.5x10<sup>6</sup> epimastigotes/mL in LIT medium. The cultures were incubated with a 20  $\mu$ M DCFH<sub>2</sub>-DA solution for 15 min at 28 °C. Then, they were spun at 3500 rpm and washed 2 times with pH 7.4 saline phosphate buffer. Cells loaded with DCFH<sub>2</sub>-DA were transferred to a Nunc® fluorescence 96-well plate, where the 3-nitrocoumarins series were added at 10  $\mu$ M. Fluorescence (excitation: 488 nm, emission: 528 nm) was recorded for 40 min on a Biotek Synergy HT spectrofluorometer. The area under the fluorescence increase curves over time was determined using Origin 8 software, the areas were normalized with the control. The results are the means  $\pm$  SD from three independent experiments.

### 2.4.5. Effect on intracellular parasites

Vero cells were detached by trypsinization, sedimented and resuspended in media containing 10% FBS. Then, 5  $\times$  10<sup>4</sup> cells were seeded into six-well plates. The cells were allowed to adhere to the bottom of the wells for 2 h and were then challenged with the parasites at a Vero cell:parasite ratio of 1:3 for 2 h, after which the supernatant was removed and the cells were exposed to the compounds or NFX at the IC<sub>50</sub> concentration, for other 24 h.

**2.4.5.1. Morphological analysis.** Vero cells were fixed in cold 90% methanol and washed with PBS and incubated with 1  $\mu$ g/mL of 4,6-diamidino-2-phenylindole (DAPI) (Molecular Probes). Then, the sections were mounted in Vectashield (Scy-Tek ACA) and observed on an epifluorescence microscope (Motic BA310; Hong Kong, China). Amastigotes were recognized by their morphology, including nuclear size and the presence of a kinetoplast, and analyzed with the MATLAB® software (Liempi et al., 2015). At least 500 cells were analyzed per condition.

### 2.5. Parallel artificial membrane permeability assays (PAMPA)

Determination of permeability in an artificial membrane of the coumarins derivatives was carried out according to the methodology described by Sierpe et al. (2017) (Sierpe et al., 2017). Donor plates contained 300  $\mu$ L of the sample at a concentration of 0.5 mM (solubilized in 30% DMSO and 70% phosphate buffer pH 7.4). Quantification of compounds was carried out by spectrophotometry in a microplate spectrophotometer (Multiskan Spectrum, Thermo Electron Co.). PAMPA assay was performed in triplicate (n = 3). Data is expressed as the means  $\pm$  SD from three independent measures.

## 2.6. Statistical analysis

Statistical analysis was performed using Graph Pad Prism 4.03 (GraphPad Software, San Diego, California USA). Data are expressed as mean  $\pm$  SD of three independent experiments. Statistical analysis was performed using one-way ANOVA with Dunnett post-test when multiple comparisons were required. Data are considered statistically significant when  $p$  less than 0.05.

## 3. Results and discussion

### 3.1. Chemistry

Compounds **1–5** were synthesized according to the scheme presented in Fig. 1a. 4-Hydroxy-3-nitrocoumarin undergoes an esterification reaction in the presence of an acid chloride, in dichloromethane and using dry pyridine, from 0 °C to room temperature. The reaction is complete after stirring overnight. The reaction mixture is then purified by flash chromatography to afford the desired compound. In order to explore the chemical space, different substituents were included at position 4 of the scaffold.

#### 3.1.1. Electrochemical studies

Electrochemical characterization of the new 3-nitrocoumarins was performed by CV in an aprotic medium. Fig. 1b shows the

cyclic voltammogram of compound **1**, the first cathodic signal (Ic), without the corresponding anodic signal, was not assigned to any particular species. Second quasi reversible peak (IIc), observed at more negative potentials, was assigned to the mono-electronic reduction of the nitro group that generates the nitro anion radical  $R-NO_2^{\cdot-}$  (Eq. (2)). This step has been described as the first step required to reduce nitro compounds. All the compounds of the series exhibited similar electrochemical behavior, which agrees with previous reports (Aravena, Figueroa, Olea-Azar, & Arán, 2010; Bollo et al., 2003; C. Olea-Azar et al., 1998; Rigol et al., 2005; Squella, Bollo, & Nunez-Vergara, 2005).

In particular, the reduction of nitroaromatic compounds in aprotic solvents has been widely described, where the first coupling is reversible. However, this is not the case for the studied series. This fact may be explained by the low stability of the anion radical formed by the substituent at 3 position of the coumarin.



On the other hand, to determine if the reduction process was controlled by an adsorption or diffusion phenomenon, logarithm of cathode peak ( $\log(I_{pc})$ ) was plotted against the logarithm of speed of process ( $\log(v)$ ) (Fig. 1c). The value of the slope indicates the process involved. For a diffusion-controlled process, the value of the slope of the curve is close to 0.5 and for a controlled adsorption process, the value is close to 1.0. Slope values for all the compounds indicate a

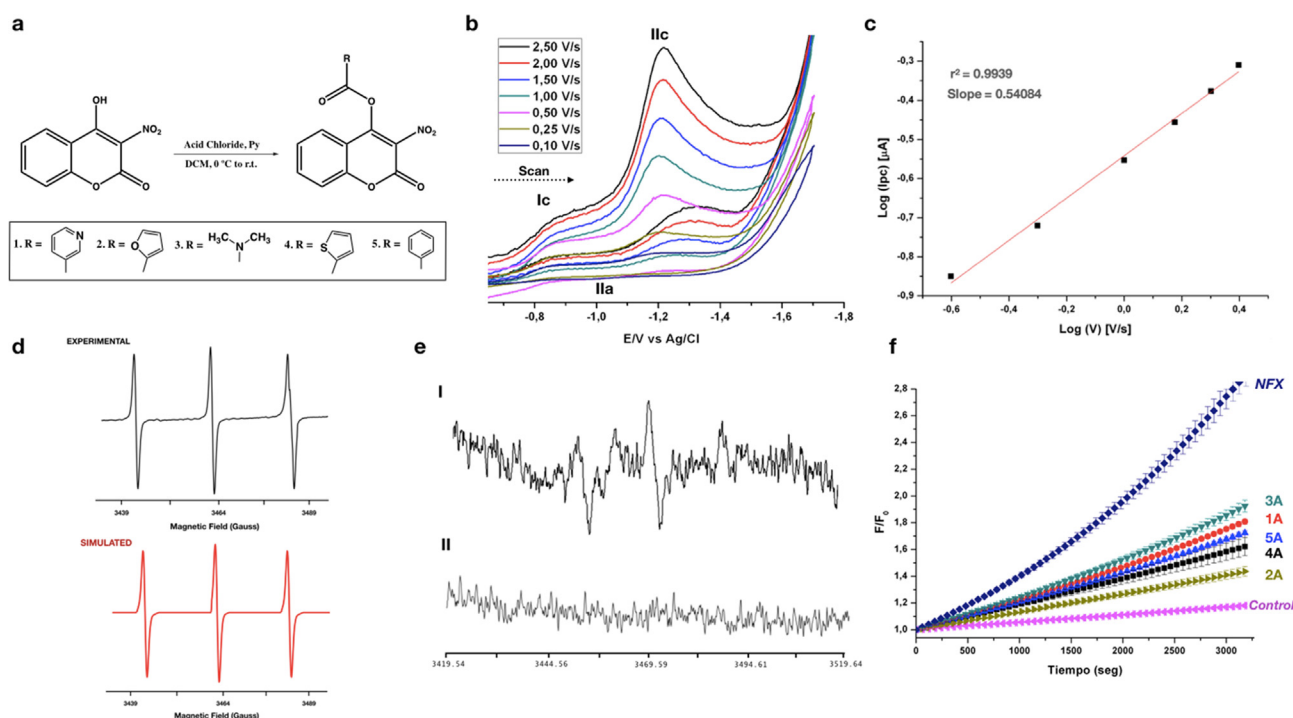


**Fig. 1** a) Synthetic methodology to afford compounds **1–5**. b) Cyclic voltammogram of compound **1** for  $v = 2.5–0.10$  V/s. c) linear relationship between  $\log I_{pc}$  versus  $\log$  scan speed ( $v$ ). d) Simulated and experimental ESR spectra of compound **1** radical electrochemically generated. e) Spectrum of spin adducts generated in *T. cruzi* epimastigote, at room temperature. I. Recorded spectrum of compound **1** with DMPO in epimastigotes and II. Control spectrum (# indicates the spin-adduct DMPO-OH and \* indicates the DMPOX adduct). f) Evaluation of ROS generation in epimastigotes at a concentration of  $10 \mu\text{M}$  of all compounds (control corresponds to parasites without addition of compound).

diffusion-controlled process without adsorptive interference on the surface of the working electrode (Nicholson & Shain, 1964; Rodríguez et al., 2008).

Cathodic and anode peak potentials of all compounds are shown in Table 1. The reduction potentials of all the coumarins were higher than NFX. Therefore, the 4 position of the acyloxy groups, together with the electron-attracting effect of the carbonyl at position 2, would hinder the reduction of the nitro group relative to BZN and NFX. These values are similar to those described by Pardo-Jimenez and co-workers for dihydropyridine-fused coumarins with a nitro group at position 7 of coumarin scaffold. In the voltammogram previously obtained by the authors, in similar conditions, a low intensity signal can be observed that is not attributed to any particular species (Pardo-Jiménez et al., 2014).

Comparing to other nitro compounds, our research group previously found similar values of reduction potential for a series of 5-nitroindazoles (compounds with high trypanocidal activity) that do not contain labile hydrogens in their structure, exhibiting a low intensity peak at less negative potentials that was not assigned (Claudio Olea-Azar et al., 2006). Likewise, Aguilera-Venegas and co-workers described for a series of 7-nitroquinoxalin-2-ones with trypanocidal activity and potential values close to 1.1 V, for compounds without labile hydrogens (Aguilera-Venegas et al., 2011).

### 3.1.2. Radical characterization by ESR

To deeply study the 3-nitrocoumarins reduction mechanism, the radical electrolytic generation was obtained by CV. The detection and characterization of these radical species was performed using ESR (Barriga-Gonzalez et al., 2015; Davies, 2016). Electrochemical reduction of substituted 3-nitrocoumarins was performed under the same conditions as for the CV, using the potentials for the formation of nitro anion radical. For all the studied compounds, a hyperfine pattern of three broad lines was obtained (Fig. 1d) that were assigned to nitro group nitrogen without the apparent delocalization of radical in the benzene ring of the coumarin. Hyperfine coupling constants were obtained by semi-empirical simulation of spectra using WinSIM 9.

The observed hyperfine pattern would indicate that the unpaired electron is centered in the nitro group, independent of substituents at position 4. Hyperfine coupling constants obtained in the ESR study of the family of 4-acyloxy-3-nitrocoumarins are shown in Table 2. According to Kolker and co-workers (Waters, 1963), the value of the hyperfine coupling constants can vary depending on the solvent used. That is because the presence of a polar solvent allows the hyperfine

**Table 2** Hyperfine coupling constants and g value (in Gauss units) of the simulated 4-acyloxy-3-nitrocoumarins free radical spectrum.

Compound	$a_N$	g-value
1	20.23	2.103
2	20.26	2.115
3	20.24	2.108
4	20.25	2.113
5	20.28	2.128

constant to considerably increase its value due to a radical-solvent interaction, causing changes in the electron density distribution in the radical. Furthermore, the width of the lines suggests the existence of smaller coupling constants that add to the high coupling constants in the spectrum. Likewise, the similarity of the g values could indicate that the series of the studied nitrocoumarins feels the same magnetic field corresponding to the nitrogen atom of the nitro group, since its g value provides information on the electronic structure of a paramagnetic center, regardless the chemical medium in which it is found.

To rationalize these results, the nucleophilic Fukui function ( $f_k^+$ ) was obtained for the neutral molecule of all the 4-acyloxy-3-nitrocoumarins. Table 3 shows that the atom with an increased possibility for a nucleophilic attack is carbon 4. That is due to electron-attracting effect of the nitro group, which can delocalize the positive charge on the ring A (Scheme 1). This effect was more noticeable in compound 3, since in position 7 of the coumarin presented the highest  $f_k^+$ .

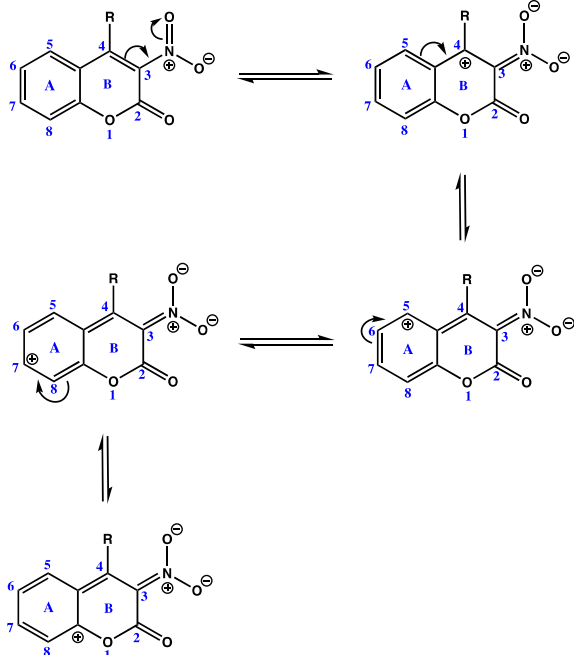
According to the above, the formation of the nitro radical would subsequently imply a higher location at carbon 4 of the coumarin scaffold. Compound 3 presented the highest  $f_k^+$ , so it would be expected that it had a lower reduction potential. However, it was compound 2 that presented the lowest reduction potential. This could be explained by the  $f_k^+$  at carbons 3' and 5', due to the influence of the furan oxygen, unlike compound 3 where the tertiary amine does not present this influence.

Delocalization in the A ring of the coumarin, which could have the unpaired electron when the nitro radicals formed, could explain the width of the lines observed in the ESR spectra, which can involve low hyperfine coupling constants of hydrogens of the ring A.

Consequently, a reduction mechanism is proposed in Scheme 1, implying the formation of a nitro anion radical

**Table 1** Electrochemical parameters in DMSO.

Compound	$E_{pc}$ II	$E_{pa}$ II	$\Delta E$	$I_{pc}$ II	$I_{pa}$ II	$I_{pa}/I_{pc}$
1	-1.20	-1.07	0.13	-0.18	-0.03	0.17
2	-1.18	-1.03	0.14	-2.39	-0.35	0.15
3	-1.19	-1.08	0.11	-0.38	-0.11	0.29
4	-1.30	-1.14	0.16	-2.69	-0.57	0.21
5	-1.24	-1.13	0.11	-0.49	-0.14	0.29
NFX	-0.88	-0.81	0.07	0.05	0.02	-0.45
BZN	-0.79	-1.14	0.35	-0.63	0.51	-0.81



**Scheme 1** Delocalization of charge density in coumarin scaffold.

and its subsequent oxidation in a reversible mechanism, which can involve redox recycling in biological systems, as it has been proposed for NFX and BZN. It should be noted that obtaining  $f_k^+$  was essential to explain the line widths observed in the ESR spectra and it turned out to be a useful tool to postulate the mechanism of action that involve radical species.

### 3.2. Biological activity

#### 3.2.1. Cytotoxic in mammalian cell

Cytotoxicity was determined in RAW 264.7 macrophage line determining the cell viability through the tetrazolium salt reduction assay. None of the compounds under study was found to interfere with the method, due to its characteristics as oxidants. All the coumarin derivatives presented  $IC_{50}$  values above  $200 \mu M$  (Table 4); thus, considering to be non-toxic against this cell line. These values were higher than those reported for the series of 3-amidocoumarins, 3-carboxamidocoumarins and hydroxy-3-arylcoumarins, except for the 7,8-dihydroxy-3-(hydroxyphenyl)coumarins, which were previously studied by the group, and also higher than that determined for NFX.

Therefore, it would be of high interest for subsequent studies to maintain the nitro group in the coumarin scaffold, modifying the substituents at position 4, to reduce the cytotoxicity comparing to the currently used drugs.

Low cytotoxicity on this cell line represents an huge advantage, since macrophages belong to the mononuclear phagocytic system, which constitute one of the main defense mechanisms of the organism against external pathogens, enabling the use of these compounds as potential trypanocidal agents.

#### 3.2.2. In vitro trypanocidal activity

Trypanocidal activity of all the compounds was evaluated on the trypomastigote form of *T. cruzi* (Dm28c), calculating the  $IC_{50}$  values for all of them. Results in Table 4 indicate that all the studied coumarins showed similar trypanocidal activity to that previously described by the group for a series of 3-amido-4-hydroxycoumarins (Moncada-Basualto et al., 2018). In that study, a compound presenting a pyridine substituent was described as the most active. This suggests that the lipophilicity of the compounds is not a predominant factor for the activity.

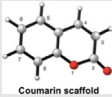
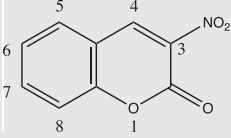
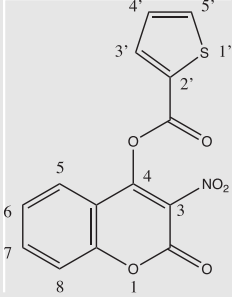
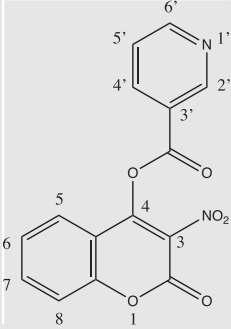
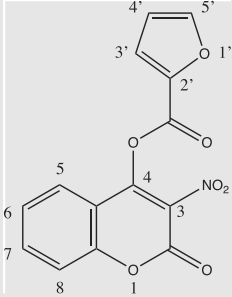
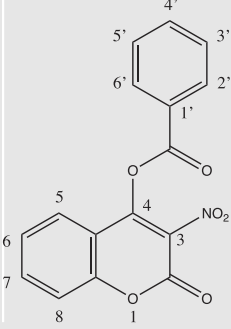
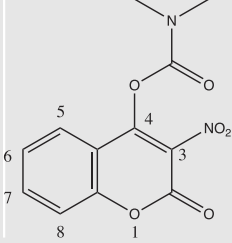
These compounds were less active than the 3-amidocoumarins also described by the group (Gutiérrez et al., 2013), which suggests that the introduction of more lipophilic substituents decreases the activity of this series of compounds. However, the presence of a nitro group in position 3 of the coumarin scaffold seems to be fundamental, since it decreases the activity against mammalian cells, possibly due to the structural similarity with NAD, which can also partially explain a possible trypanocidal mechanism of action by inhibition of the enzyme GAPDH.

Another trypanocidal mechanism of action associated with the nitro compounds may be based on the generation of oxidative stress. Mammalian cells have more efficient endogenous antioxidant mechanisms than *T. cruzi*. Nitroreductases are responsible for reducing the nitro group, generating the nitro anion radical, triggering a series of chain reactions or products that cause damage to the parasite. However, it appears that the trypanocidal activity is not correlated with the reduction potentials of the compounds, unlike that described for other trypanocidal nitro-compounds (Claudio Olea-Azar et al., 2006; Rodríguez et al., 2008). Thus, the trypanocidal action may not be observed due to the generation of oxidative stress through the formation of a nitroanion radical.

To associate the trypanocidal activity with the permeability of the membrane of the compounds under study, a PAMPA test model was used (Kansy, Senner, & Gubernator, 1998). It is worth mentioning that the PAMPA technique is a preliminary test that allows an indication of a possible passive diffusion of the compound in artificial membrane and thus determine its physicochemical properties. Of the entire series of compounds studied, it was observed that compound 3 was the only one that presented diffusion through the membrane with an effective permeability ( $P_e$ ) of  $3.2 \times 10^{-7} \text{ cm/s}$  (Table 5), which it was lower than previously described by the group for a series of coumarins in a more complex membrane model (Maria João Matos et al., 2015).

Compound 3 is less lipophilic due to the tertiary amine and the smaller volume of the substituent, which can explain a higher diffusion in this membrane model. This hypothesis can be partially corroborated by the high association percentages of the most lipophilic compounds in the artificial membrane. Likewise, it must be taken into account that these values cannot be directly correlated with the trypanocidal activity, since both the parasite and the mammalian cells have cell membranes that are lipidic bilayers with different compositions (glycoproteins, mucins, transialidase, among others) (de Souza, 2009). Therefore, another type of diffusion, such as active, may be involved. In this case, several transporters, such as proteins, can help the diffusion of the compound.

**Table 3** Fukui indices ( $f_k^+$ ) for 4-acyloxy-3-nitrocoumarins computed at B3LYP-D3/Def2TZVP//Def2SVP level.

Compound		Fukui Index		Compound		Fukui Index	
 Coumarin scaffold							
		O <sub>1</sub> 0.048 O <sub>2</sub> 0.117 C <sub>4</sub> 0.159 C <sub>5</sub> 0.089 C <sub>7</sub> 0.126				O <sub>2</sub> 0.061 O <sub>3</sub> 0.096 O <sub>4</sub> 0.076 O <sub>6</sub> 0.051 C <sub>4</sub> 0.114 C <sub>5</sub> 0.053 C <sub>7</sub> 0.079 C <sub>2'</sub> 0.064	
		O <sub>2</sub> 0.068 O <sub>3</sub> 0.105 O <sub>4</sub> 0.093 C <sub>3</sub> 0.051 C <sub>4</sub> 0.138 C <sub>5</sub> 0.066 C <sub>7</sub> 0.092 C <sub>2'</sub> 0.058				O <sub>2</sub> 0.067 O <sub>3</sub> 0.120 O <sub>4</sub> 0.113 C <sub>4</sub> 0.151 C <sub>5</sub> 0.077 C <sub>7</sub> 0.103	
		O <sub>2</sub> 0.065 O <sub>3</sub> 0.100 O <sub>4</sub> 0.085 S <sub>3'</sub> 0.079 C <sub>4</sub> 0.129 C <sub>5</sub> 0.061 C <sub>7</sub> 0.086 C <sub>2'</sub> 0.052				O <sub>2</sub> 0.063 O <sub>3</sub> 0.098 O <sub>4</sub> 0.081 C <sub>4</sub> 0.122 C <sub>5</sub> 0.058 C <sub>7</sub> 0.083	

### 3.2.3. Determination of intracellular parasites

Most of the compounds with potential trypanocidal activity are tested on the extracellular form of the parasite, evaluating their efficacy in the acute phase of the disease. However, the evaluation of the activity on the intracellular form would account for the efficacy in the chronic phase of the disease.

In this case, DAPI staining was used, which recognizes the presence of intracellular parasites as well as their nuclear and kinetoplasmic size (Fig. 2a, c, e and g), due to the great capacity of this molecule to bind nucleic acids, generating a blue fluorescence stain.

In addition, we assayed the effect of the compounds **1** and **2** on mammalian cells infected with intracellular amastigotes. Vero cells infected previously with the parasite were incubated in the presence and absence of the selected compounds or NFX, at their respective IC<sub>50</sub> values.

Compound **1** significantly decreased ( $p \leq 0.0001$ ) the percentage of infected cells in a lower way than NFX (Fig. 2a and 2b). Compound **2** did not reduce the percentage of infection of VERO cells. Finally, compound **1** did not significantly decrease the number of amastigotes per cell, comparing to the infection control (Fig. 2e and 2f).

**Table 4** *In vitro* cytotoxicity in murine RAW 264.7 macrophages (IC<sub>50</sub>) and trypanocidal activity against trypanomastigote strain (IC<sub>50</sub>).

Compound	Trypomastigote	RAW 264.7	SI <sup>c</sup>
	IC <sub>50</sub> /μM	IC <sub>50</sub> /μM	
<b>1</b>	137.4 ± 1.3	> 200 <sup>a</sup>	> 1.46
<b>2</b>	237.6 ± 2.1	> 200 <sup>a</sup>	> 0.84
<b>3</b>	212.9 ± 1.6	> 200 <sup>a</sup>	> 0.94
<b>4</b>	223.3 ± 1.8	> 200 <sup>a</sup>	> 0.90
<b>5</b>	187.7 ± 1.4	> 200 <sup>a</sup>	> 1.07
<b>NFX</b>	10.0 ± 0.4	263.4 <sup>b</sup>	> 26.34

<sup>a</sup> The highest studied concentration was 200 μM, since the compounds are active between 10 and 100 μM. <sup>b</sup> reference value obtained from Robledo et al 2017. <sup>c</sup>SI: selective index, (IC<sub>50</sub> raw 264.7/IC<sub>50</sub> parasite). All experiments were carried out in triplicate, and the data represent the mean values (± S.D.).

Although the trypanocidal activity of the studied 3-nitrocoumarins is low, comparing to the other coumarins studied by the group, it was possible to determine that compound **1** reduces the number of infected cells. The new data add value to the potential use of trypanocidal coumarins in the treatment of Chagas disease, considering that a limit in the efficacy of anti-chagasic drugs is the low activity in infective forms of *T. cruzi*.

### 3.3. Detection of radical species

#### 3.3.1. ESR spin trapping

Free radical formation in the epimastigote form of *T. cruzi* was carried out to determine whether oxidative stress is a possible mechanism of action of the substituted 3-nitrocoumarins. ESR was used with the spin trapping technique and DMPO was used as a spin trap, since it can cross cell membranes and react with free radicals focused on oxygen and carbon, thus, differentiating between the spectra obtained (Aguilera-Venegas et al., 2013; Aguilera-Venegas & Speisky, 2014; Barriga-Gonzalez et al., 2015). Fig. 1e shows the ESR-generated representative spectra. It was observed that all the compounds under study generated the same hyperfine coupling pattern (Aguilera-Venegas et al., 2013; Moncada-Basualto et al., 2018; Claudio Olea-Azar et al., 2003). This decomposition is due to the previous formation of the spin adduct between DMPO and the hydroxyl radical, which was then DMPOx, through the mechanism proposed in Scheme 2.

Detection of radical species would indicate that one of the mechanisms of action for this type of compound involves the generation of oxidative stress, which could be generated by the

**Table 5** Association and diffusion percentages to artificial membrane.

Compounds	% Association	% Diffusion	Pe/cms <sup>-1</sup>
<b>1</b>	98.9 ± 0.1	–	–
<b>2</b>	6.1 ± 0.1	–	–
<b>3</b>	27.7 ± 0.5	1.67 ± 0.3	3.2 × 10 <sup>-7</sup> ± 0.2
<b>4</b>	40.8 ± 0.5	–	–
<b>5</b>	19.2 ± 0.7	–	–

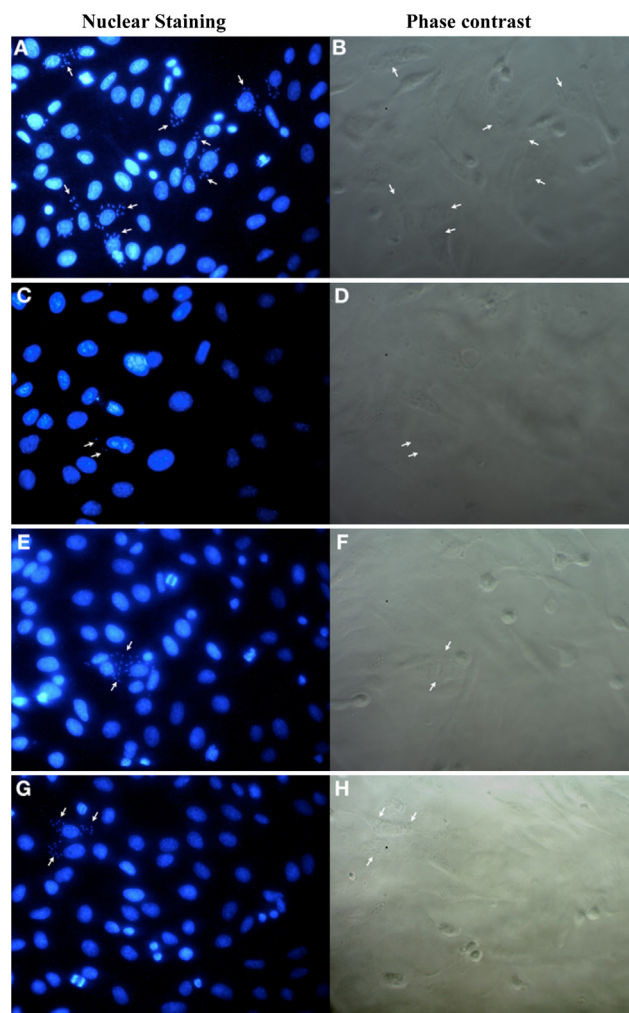
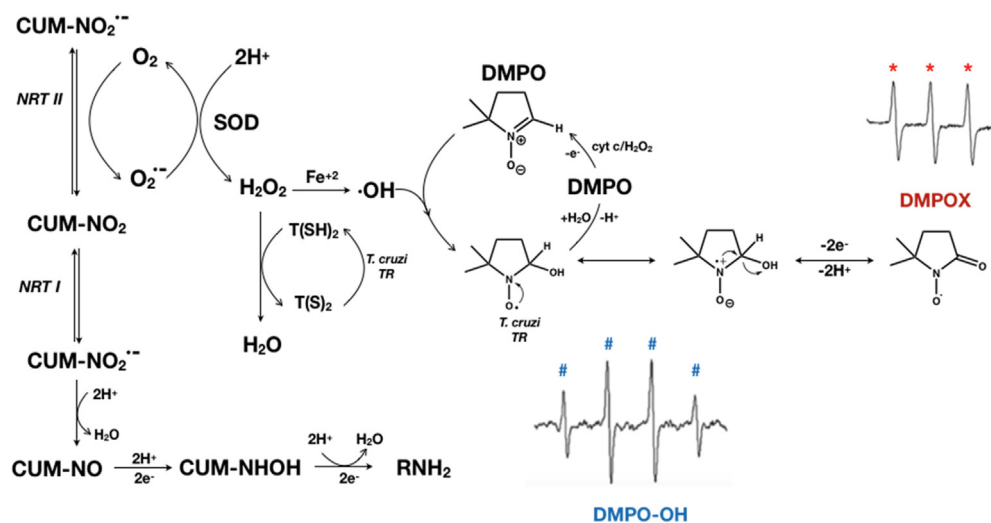


**Fig. 2** Infected Vero cells with *T. cruzi* amastigotes. The arrows show Vero cells nuclei and intracellular amastigotes. Scale bar: 10 μm. <sup>A</sup>Control with nuclear staining with DAPI, <sup>B</sup> Phase contrast control, <sup>C</sup> NFX with nuclear staining with DAPI, <sup>D</sup> NFX with phase contrast, <sup>E</sup> Compound **1** nuclear staining with DAPI, <sup>F</sup> Compound **1** with phase contrast, <sup>G</sup> Compound **2** nuclear staining with DAPI, <sup>H</sup> Compound **2** with phase contrast.

nitro group. Likewise, it is worth mentioning that the use of a spin trapping technique is essential for detection and characterization of free radicals in whole cells, which has made it possible to postulate this type of trypanocidal mechanism of action.

#### 3.3.2. Determination of intracellular oxidative stress

To quantify the generation of radical species in *T. cruzi* epimastigotes, determination of intracellular free radicals was performed based on the quantification of dichlorofluorescein probe (DCF). All the compounds managed to penetrate the cell membrane, generating an increase in the fluorescence intensity (Fig. 1f). Compound **3** presented the highest increase in fluorescence intensity related to an increase in the intracellular free radical concentration. This effect was less than that found for NFX. These results are similar to those obtained through PAMPA, where compound **3** presented higher membrane permeability. This suggests that the trypanocidal mech-



**Scheme 2** Proposed mechanism for the generation of radical species in *T. cruzi* epimastigotes.

anism of action may not involve the generation of oxidative stress as the only route of action.

The ROS generation assay indicates that all the compounds can permeate the parasite membrane by different mechanisms, unlike that found by the PAMPA assay. Therefore, the ROS generation assay would be more useful for the study of this type of compounds, since it provides information about membrane permeability and evaluation of oxidative stress *in vitro* in different types of cells.

Therefore, for further studies, it would be interesting to study a series of compounds that maintain the 3-nitrocoumarin scaffold, presenting different substituents at position 4, with similar lipophilicity to compound **1**. It would be also interesting to evaluate other potential mechanisms of action.

#### 4. Conclusions

Voltammetric and ESR studies suggested that the formation of a nitro radical anion is possible, which would emulate the enzymatic function within the parasite. The Fukui index provided additional evidence of the relevance of the nitro group at position 3, whose electron withdrawing effects can delocalize the charge density of the coumarin scaffold. Regarding the trypanocidal activity, it was established that the compounds present low trypanocidal activity. This may be related to the formation of intracellular free radicals, evidenced through the tests of spin trapping and formation of intracellular ROS. It is postulated that the mechanism of trypanocidal action in the studied series would not only be via oxidative stress, given the low correlation of these parameters. Suggested mechanisms involve essential enzymes for the survival of the parasite. The membrane permeability test suggests that high lipophilic compounds are mostly retained in the membrane. In this case, there is no direct relationship between the biological activity observed and the percentage of diffusion of the compounds. Finally, the decrease in cells infected with parasites in the amastigote form suggests that the introduction of the pyridine substituent is essential to decrease the infection rate. Therefore, in future studies the synthesis and biological evaluation of coumarins with nitrogen-containing heterocycles in different positions of the scaffold would be interesting to

improve the bioavailability and enhance the use of this type of compounds as trypanocidal agents.

#### Conflict of interest

The authors declare no conflict of interest, financial or otherwise.

#### Acknowledgements

This project was partially supported by the University of Porto and University of Santiago de Compostela. MJM would like to thank Xunta de Galicia (Galician Plan of Research, Innovation and Growth 2011–2015, Plan I2C, ED481B 2014/086–0 and ED481B 2018/007) and Fundação para a Ciência e Tecnologia (CEECIND/02423/2018 and UIDB/00081/2020). Authors would like to thank Prof. Lourdes Santana for her scientific support. Authors would like to thank the use of RIAIDT-USC analytical facilities. FS would like to thank FONDECYT 1190340 and REDES170126, COA would like to thank FONDECYT 1190340, JDM would like to thank FONDECYT 1170126 and ANID/PCI REDES 170126, and MMB would like to thank FONDECYT Postdoctoral 3190449.

#### References

- Aguilera-Venegas, B., Olea-Azar, C., Arán, V.J., Speisky, H., 2013. Indazoles: a new top seed structure in the search of efficient drugs against *Trypanosoma cruzi*. *Future Med. Chem.* 5 (15), 1843–1859. <https://doi.org/10.4155/fmc.13.144>.
- Aguilera-Venegas, B., Olea-Azar, C., Norambuena, E., Arán, V.J., Mendizábal, F., Lapier, M., López-Muñoz, R., 2011. ESR, electrochemical, molecular modeling and biological evaluation of 4-substituted and 1,4-disubstituted 7-nitroquinoxalin-2-ones as potential anti-*Trypanosoma cruzi* agents. *Spectrochim. Acta - A: Mol. Biomol. Spectroscopy* 78 (3), 1004–1012. <https://doi.org/10.1016/j.saa.2010.12.017>.
- Aguilera-Venegas, B., Speisky, H., 2014. Identification of the transition state for fast reactions: The trapping of hydroxyl and methyl radicals by DMPO - A DFT approach. *J. Mol. Graph. Model.* 52, 57–70. <https://doi.org/10.1016/j.jmgm.2014.06.006>.

- Aravena, M.C., Figueroa, R., Olea-Azar, C., Arán, V.J., 2010. ESR, electrochemical and ORAC studies of nitro compounds with potential antiprotozoal activity. *J. Chil. Chem. Soc.* 55 (2), 244–249. <https://doi.org/10.4067/s0717-97072010000200022>.
- Barriga-Gonzalez, G., Olea-Azar, C., Zuniga-Lopez, M., Folch-Cano, C., Aguilera-Venegas, B., Porcal, W., Cerecetto, H., 2015. Spin trapping: an essential tool for the study of diseases caused by oxidative stress. *Curr. Top. Med. Chem.* 15 (5), 484–495. <https://doi.org/10.2174/1568026615666150206155108>.
- Bisby, R.H., Brooke, R., Navaratnam, S., 2008. Effect of antioxidant oxidation potential in the oxygen radical absorption capacity (ORAC) assay. *Food Chem.* 108 (3), 1002–1007. <https://doi.org/10.1016/j.foodchem.2007.12.012>.
- Boiani, M., Piacenza, L., Hernández, P., Boiani, L., Cerecetto, H., González, M., Denicola, A., 2010. Mode of action of Nifurtimox and N-oxide-containing heterocycles against *Trypanosoma cruzi*: Is oxidative stress involved?. *Biochem. Pharmacol.* 79 (12), 1736–1745. <https://doi.org/10.1016/j.bcp.2010.02.009>.
- Bollo, S., Núñez-Vergara, L.J., Martínez, C., Chauviere, G., Périé, J., Squella, J.A., 2003. Voltammetric study of nitro radical anion generated from some nitrofurans compounds of pharmacological significance. *Electroanalysis* 15 (1), 19–25. <https://doi.org/10.1002/elan.200390000>.
- Bonney, K.M., 2014. Chagas disease in the 21st Century: a public health success or an emerging threat?. *Parasite* 21. <https://doi.org/10.1051/parasite/2014012>.
- Borges, F., Roleira, F., Milhazes, N., Santana, L., Uriarte, E., 2005. Simple coumarins and analogues in medicinal chemistry: occurrence, synthesis and biological activity. *Curr. Med. Chem.* 12 (8), 887–916. <https://doi.org/10.2174/0929867053507315>.
- Davies, M.J., 2016. Detection and characterisation of radicals using electron paramagnetic resonance (EPR) spin trapping and related methods. *Methods* 109, 21–30. <https://doi.org/10.1016/j.ymeth.2016.05.013>.
- de Souza, W., 2009. Structural organization of *Trypanosoma cruzi*. *Mem. Inst. Oswaldo Cruz* 104 (SUPPL. 1), 89–100. <https://doi.org/10.1590/s0074-02762009000900014>.
- Duling, D.R., 1994. Simulation of multiple isotropic spin-trap EPR spectra. *J. Magn. Reson., Ser B* 104, 105–110. <https://doi.org/10.1006/jmrb.1994.1062>.
- Estani, S.S., Segura, E.L., Ruiz, A.M., Velazquez, E., Porcel, B.M., Yamptis, C., 1998. Efficacy of chemotherapy with benznidazole in children in the indeterminate phase of Chagas' disease. *Am. J. Trop. Med. Hyg.* 59 (4), 526–529. <https://doi.org/10.4269/ajtmh.1998.59.526>.
- Fernández, M.L., Marson, M.E., Ramirez, J.C., Mastrantonio, G., Schijman, A.G., Altchek, J., Bournissen, F.G., 2016. Pharmacokinetic and pharmacodynamic responses in adult patients with chagas disease treated with a new formulation of benznidazole. *Mem. Inst. Oswaldo Cruz* 111 (3), 218–221. <https://doi.org/10.1590/0074-02760150401>.
- Figueroa-Guinez, R., Matos, M., Vazquez-Rodriguez, S., Santana, L., Uriarte, E., Borges, F., Maya, J., 2015. Interest of Antioxidant Agents in Parasitic Diseases. The Case Study of Coumarins. *Curr. Top. Med. Chem.* 15 (9), 850–856. <https://doi.org/10.2174/1568026615666150220113155>.
- Frisch MJ, Trucks GW, Schlegel HB, Scuseria GE, Robb MA, Cheeseman JR, Scalmani G, Barone V, Petersson GA, Nakatsuji H, Li X, Caricato M, Marenich AV, Bloino J, Janesko BG, Gomperts R, Mennucci B, Hratchian HP, Ortiz JV, Izmaylov AF, Sonnenberg JL, W., & DJ, F. (2009). *Gaussian 09 Rev. B.01*. 2009.
- Govêa, K.P., Pereira, R.S.T., De Assis, M.D.O., Alves, P.I., Brancaglioni, G.A., Toyota, A.A.E., Barbosa, S., 2020. Allelochemical activity of eugenol-derived coumarins on *lactuca sativa* L. *Plants* 9 (4), 1–17. <https://doi.org/10.3390/plants9040533>.
- Guíñez, R.F., Matos, M.J., Vazquez-Rodriguez, S., Santana, L., Uriarte, E., Olea-Azar, C., Maya, J.D., 2013. Synthesis and evaluation of antioxidant and trypanocidal properties of a selected series of coumarin derivatives. *Future Med. Chem.* 5 (16), 1911–1922. <https://doi.org/10.4155/FMC.13.147>.
- Hadjipavlou-Litina, D., Litinas, K., Kontogiorgis, C., 2008. The anti-inflammatory effect of coumarin and its derivatives. *AntiInflammatory Antiallergy Agents Med Chem* 6 (4), 293–306. <https://doi.org/10.2174/187152307783219989>.
- Iaroshenko, V.O., Erben, F., Mkrtchyan, S., Hakobyan, A., Vilches-Herrera, M., Dudkin, S., Langer, P., 2011. 4-Chloro-3-(trifluoroacetyl)- and 4-chloro-3-(methoxalyl)coumarins as novel and efficient building blocks for the regioselective synthesis of 3,4-fused coumarins. *Tetrahedron* 67 (41), 7946–7955. <https://doi.org/10.1016/j.tet.2011.08.030>.
- Irigoien, F., Cibils, L., Comini, M.A., Wilkinson, S.R., Flohé, L., Radi, R., 2008. Insights into the redox biology of *Trypanosoma cruzi*: Trypanothione metabolism and oxidant detoxification. *Free Radical Biol. Med.* 45 (6), 733–742. <https://doi.org/10.1016/j.freeradbiomed.2008.05.028>.
- Jameel, E., Umar, T., Kumar, J., Hoda, N., 2016. Coumarin: a privileged scaffold for the design and development of antineurodegenerative agents. *Chem. Biol. Drug Des.* 87 (1), 21–38. <https://doi.org/10.1111/cbdd.12629>.
- Kansy, M., Senner, F., & Gubernator, K., 1998. Screening : Parallel Artificial Membrane Permeation Assay in the Description of. *J. Medicinal Chemistry*, 41(7), 1007–1010.
- Lazarin-Bidóia, D., Desoti, V.C., Ueda-Nakamura, T., Dias Filho, B.P., Nakamura, C.V., Silva, S.O., 2013. Further evidence of the trypanocidal action of eupomatenoide-5: Confirmation of involvement of reactive oxygen species and mitochondria owing to a reduction in trypanothione reductase activity. *Free Radical Biol. Med.* 60, 17–28. <https://doi.org/10.1016/j.freeradbiomed.2013.01.008>.
- Liempi, A., Castillo, C., Cerda, M., Droguett, D., Duaso, J., Barahona, K., Kemmerling, U., 2015. *Trypanosoma cruzi* infectivity assessment in “in vitro” culture systems by automated cell counting. *Acta Trop.* 143, 47–50. <https://doi.org/10.1016/j.actatropica.2014.12.006>.
- Malik, L.H., Singh, G.D., Amsterdam, E.A., 2015. Chagas heart disease: an update. *Am. J. Med.* 128 (11), 1251.e7–1251.e9. <https://doi.org/10.1016/j.amjmed.2015.04.036>.
- Matos, Maria João, Pérez-Cruz, F., Vazquez-Rodriguez, S., Uriarte, E., Santana, L., Borges, F., Olea-Azar, C., 2013. Remarkable antioxidant properties of a series of hydroxy-3-arylcoumarins. *Bioorg. Med. Chem.* 21 (13), 3900–3906. <https://doi.org/10.1016/j.bmc.2013.04.015>.
- Matos, Maria João, Rodríguez-Enríquez, F., Vilar, S., Santana, L., Uriarte, E., Hripsak, G., Viña, D., 2015. Potent and selective MAO-B inhibitory activity: amino- versus nitro-3-arylcoumarin derivatives. *Bioorg. Med. Chem. Lett.* 25 (3), 642–648. <https://doi.org/10.1016/j.bmcl.2014.12.001>.
- Matos, Maria João, Vilar, S., García-Morales, V., Tatonetti, N.P., Uriarte, E., Santana, L., Viña, D., 2014. Insight into the functional and structural properties of 3-arylcoumarin as an interesting scaffold in monoamine oxidase B inhibition. *ChemMedChem* 9 (7), 1488–1500. <https://doi.org/10.1002/cmdc.201300533>.
- Matos, Maria João, Viña, D., Janeiro, P., Borges, F., Santana, L., Uriarte, E., 2010. New halogenated 3-phenylcoumarins as potent and selective MAO-B inhibitors. *Bioorg. Med. Chem. Lett.* 20 (17), 5157–5160. <https://doi.org/10.1016/j.bmcl.2010.07.013>.
- Matos, Maria Joao, Viña, D., Picciani, C., Orallo, F., Santana, L., Uriarte, E., 2009. Synthesis and evaluation of 6-methyl-3-phenylcoumarins as potent and selective MAO-B inhibitors. *Bioorg. Med. Chem. Lett.* 19 (17), 5053–5055. <https://doi.org/10.1016/j.bmcl.2009.07.039>.
- Maya, J.D., Cassels, B.K., Iturriaga-Vásquez, P., Ferreira, J., Faúndez, M., Galanti, N., Morello, A., 2007. Mode of action of natural and synthetic drugs against *Trypanosoma cruzi* and their interaction with the mammalian host. *Comparat. Biochem. Physiol. – A Mol. Integrative Physiol.* 146 (4), 601–620. <https://doi.org/10.1016/j.cbpa.2006.03.004>.

- Moncada-Basualto, M., Lapier, M., Maya, J.D., Matsuhira, B., Olea-Azar, C., Delogu, G.L., Matose, M.J., 2018. Evaluation of Trypanocidal and Antioxidant Activities of a Selected Series of 3-amidocoumarins. *Med. Chem.* 14 (6), 573–584. <https://doi.org/10.2174/1573406414666180419113437>.
- Mosmann, T., 1983. Rapid colorimetric assay for cellular growth and survival: Application to proliferation and cytotoxicity assays. *J. Immunol. Methods* 65 (1–2), 55–63. [https://doi.org/10.1016/0022-1759\(83\)90303-4](https://doi.org/10.1016/0022-1759(83)90303-4).
- Muñoz, A., Fonseca, A., Matos, M.J., Uriarte, E., Santana, L., Borges, F., Olea Azar, C., 2016. Evaluation of antioxidant and antitrypanosomal properties of a selected series of synthetic 3-carboxamidocoumarins. *ChemistrySelect* 1 (15), 4957–4964. <https://doi.org/10.1002/slct.201601336>.
- Nicholson, R.S., Shain, I., 1964. Stationary electrode polarography. *Anal. Chem.* 36 (4), 706–723.
- Olea-Azar, C., Atria, A.M., Mendizabal, F., Di Maio, R., Seoane, G., Cerecetto, H., 1998. Cyclic voltammetry and electron paramagnetic resonance studies of some analogues of nifurtimox. *Spectrosc. Lett.* 31 (1), 99–109. <https://doi.org/10.1080/00387019808006764>.
- Olea-Azar, Claudio, Cerecetto, H., Gerpe, A., González, M., Arán, V. J., Rigol, C., Opazo, L., 2006. ESR and electrochemical study of 5-nitroindazole derivatives with antiprotozoal activity. *Spectrochim. Acta - A: Mol. Biomol. Spectroscopy* 63 (1), 36–42. <https://doi.org/10.1016/j.saa.2005.04.011>.
- Olea-Azar, Claudio, Rigol, C., Mendizabal, F., Morello, A., Maya, J. D., Moncada, C., Cerecetto, H., 2003. ESR spin trapping studies of free radicals generated from nitrofurantoin derivative analogues of nifurtimox by electrochemical and Trypanosoma cruzi reduction. *Free Radical Res.* 37 (9), 993–1001. <https://doi.org/10.1080/10715760310001598141>.
- Paiva, C.N., Medei, E., Bozza, M.T., 2018. ROS and Trypanosoma cruzi: Fuel to infection, poison to the heart. *PLoS Pathog.* 14 (4), 1–19. <https://doi.org/10.1371/journal.ppat.1006928>.
- Pardo-Jiménez, V., Barrientos, C., Pérez-Cruz, K., Navarrete-Encina, P.A., Olea-Azar, C., Nuñez-Vergara, L.J., Squella, J.A., 2014. Synthesis and electrochemical oxidation of hybrid compounds: dihydropyridine-fused coumarins. *Electrochim. Acta* 125, 457–464. <https://doi.org/10.1016/j.electacta.2014.01.137>.
- Pérez-Cruz, F., Serra, S., Delogu, G., Lapier, M., Maya, J.D., Olea-Azar, C., Uriarte, E., 2012. Antitrypanosomal and antioxidant properties of 4-hydroxycoumarins derivatives. *Bioorg. Med. Chem. Lett.* 22 (17), 5569–5573. <https://doi.org/10.1016/j.bmcl.2012.07.013>.
- Pérez-Cruz, K., Moncada-Basualto, M., Morales-Valenzuela, J., Barriga-González, G., Navarrete-Encina, P., Nuñez-Vergara, L., Olea-Azar, C., 2018. Synthesis and antioxidant study of new polyphenolic hybrid-coumarins. *Arabian J. Chem.* 11 (4), 525–537. <https://doi.org/10.1016/j.arabj.2017.05.007>.
- Pérez-Molina, J.A., Molina, I., 2018. Chagas disease. *The Lancet* 391 (10115), 82–94. [https://doi.org/10.1016/S0140-6736\(17\)31612-4](https://doi.org/10.1016/S0140-6736(17)31612-4).
- Rassi, A., Rassi, A., Marcondes de Rezende, J., 2012. American Trypanosomiasis (Chagas Disease). *Infect. Dis. Clin. North Am.* 26 (2), 275–291. <https://doi.org/10.1016/j.idc.2012.03.002>.
- Razavi, B.M., Arasteh, E., Imenshahidi, M., Iranshahi, M., 2015. Antihypertensive effect of auraptene, a monoterpene coumarin from the genus Citrus, upon chronic administration. *Iranian J. Basic Med. Sci.* 18 (2), 153–158. <https://doi.org/10.22038/ijbms.2015.4018>.
- Reed, A.E., Weinstock, R.B., Weinhold, F., 1985. Natural population analysis. *J. Chem. Phys.* 83 (2), 735–746. <https://doi.org/10.1063/1.449486>.
- Ribeiro, V., Dias, N., Paiva, T., Hagström-Bex, L., Nitz, N., Pratesi, R., & Hecht, M. (2020). Current trends in the pharmacological management of Chagas disease. *Int. J. Parasitol.: Drugs Drug Resist.* 12(August 2019), 7–17. [10.1016/j.ijpddr.2019.11.004](https://doi.org/10.1016/j.ijpddr.2019.11.004).
- Rigol, C., Olea-Azar, C., Mendizabal, F., Otero, L., Gambino, D., González, M., Cerecetto, H., 2005. Electrochemical and ESR study of 5-nitrofuranyl-containing thiosemicarbazones antiprotozoal drugs. *Spectrochimica Acta - A: Mol. Biomol. Spectroscopy* 61 (13–14), 2933–2938. <https://doi.org/10.1016/j.saa.2004.11.003>.
- Riveiro, M., De Kimpe, N., Moglioni, A., Vazquez, R., Monczor, F., Shayo, C., Davio, C., 2010. Coumarins: old compounds with novel promising therapeutic perspectives. *Curr. Med. Chem.* 17 (13), 1325–1338. <https://doi.org/10.2174/092986710790936284>.
- Robledo-O’Ryan, N., Moncada-Basualto, M., Mura, F., Olea-Azar, C., Matos, M.J., Vazquez-Rodríguez, S., Maya, J.D., 2017. Synthesis, antioxidant and antichagasic properties of a selected series of hydroxy-3-aryl coumarins. *Bioorg. Med. Chem.* 25 (2), 621–632. <https://doi.org/10.1016/j.bmc.2016.11.033>.
- Rodríguez-Hernández, K. D., Martínez, I., Agredano-Moreno, L. T., Jiménez-García, L. F., Reyes-Chilpa, R., & Espinoza, B. (2019). Coumarins isolated from Calophyllum brasiliense produce ultrastructural alterations and affect in vitro infectivity of Trypanosoma cruzi. *Phytomedicine*, 61(November 2017), 152827. [10.1016/j.phymed.2019.152827](https://doi.org/10.1016/j.phymed.2019.152827).
- Rodríguez-Hernández, K.D., Martínez, I., Reyes-Chilpa, R., Espinoza, B., 2020. Mamea type coumarins isolated from Calophyllum brasiliense induced apoptotic cell death of Trypanosoma cruzi through mitochondrial dysfunction, ROS production and cell cycle alterations. *Bioorg. Chem.* 100. <https://doi.org/10.1016/j.bioorg.2020.103894> 103894.
- Rodríguez, J., Olea-Azar, C., Barriga, G., Folch, C., Gerpe, A., Cerecetto, H., González, M., 2008. Comparative spectroscopic and electrochemical study of nitroindazoles: 3-Alcoxy, 3-hydroxy and 3-oxo derivatives. *Spectrochimica Acta - A: Mol. Biomolecular Spectroscopy* 70 (3), 557–563. <https://doi.org/10.1016/j.saa.2007.07.052>.
- Santos, S.S., de Araújo, R.V., Giarolla, J., Seoud, O. El, Ferreira, E.I., 2020. Searching for drugs for Chagas disease, leishmaniasis and schistosomiasis: a review. *Int. J. Antimicrob. Agents* 55, (4). <https://doi.org/10.1016/j.ijantimicag.2020.105906> 105906.
- Sierpe, R., Noyong, M., Simon, U., Aguayo, D., Huerta, J., Kogan, M.J., Yutronic, N., 2017. Construction of 6-thioguanine and 6-mercaptopurine carriers based on cyclodextrins and gold nanoparticles. *Carbohydr. Polym.* 177 (April), 22–31. <https://doi.org/10.1016/j.carbpol.2017.08.102>.
- Soares, F.G.N., Goëthel, G., Kagami, L.P., Das Neves, G.M.H., Sauer, E., Birriel, E., Eifler-Lima, V.L., 2019. Novel coumarins active against Trypanosoma cruzi and toxicity assessment using the animal model Caenorhabditis elegans. *BMC Pharmacol. Toxicol.* 20 (Suppl 1), 1–13. <https://doi.org/10.1186/s40360-019-0357-z>.
- Souza, W., 2005. Basic cell biology of Trypanosoma cruzi. *Curr. Pharm. Des.* 8 (4), 269–285. <https://doi.org/10.2174/1381612023396276>.
- Squella, J., Bollo, S., Nunez-Vergara, L., 2005. Recent developments in the electrochemistry of some nitro compounds of biological significance. *Curr. Org. Chem.* 9 (6), 565–581. <https://doi.org/10.2174/1385272053544380>.
- Teixeira, A.R.L., Hecht, M.M., Guimaro, M.C., Sousa, A.O., Nitz, N., 2011. Pathogenesis of chagas’ disease: parasite persistence and autoimmunity. *Clin. Microbiol. Rev.* 24 (3), 592–630. <https://doi.org/10.1128/CMR.00063-10>.
- Uliassi, E., Fiorani, G., Krauth-Siegel, R.L., Bergamini, C., Fato, R., Bianchini, G., Bolognesi, M.L., 2017. Crassiflorone derivatives that inhibit Trypanosoma brucei glyceraldehyde-3-phosphate dehydrogenase (TbGAPDH) and Trypanosoma cruzi trypanothione reductase (TcTR) and display trypanocidal activity. *Eur. J. Med. Chem.* 141, 138–148. <https://doi.org/10.1016/j.ejmech.2017.10.005>.

- Vazquez-Rodriguez, S., Figueroa-Guñez, R., Matos, M.J., Santana, L., Uriarte, E., Lapier, M., Olea-Azar, C., 2013. Synthesis of coumarin-chalcone hybrids and evaluation of their antioxidant and trypanocidal properties. *MedChemComm* 4 (6), 993–1000. <https://doi.org/10.1039/c3md00025g>.
- Waters, A. (1963). 1136 216. (1136), 1136–1141.
- Wilkinson, S.R., Taylor, M.C., Horn, D., Kelly, J.M., Cheeseman, I., 2008. A mechanism for cross-resistance to nifurtimox and benznidazole in trypanosomes. *PNAS* 105 (13), 5022–5027. <https://doi.org/10.1073/pnas.0711014105>.
- Yang, W., Mortier, W.J., 1986. The use of global and local molecular parameters for the analysis of the gas-phase basicity of amines. *J. Am. Chem. Soc.* 108 (19), 5708–5711. <https://doi.org/10.1021/ja00279a008>.
- Zingales, B., Miles, M.A., Campbell, D.A., Tibayrenc, M., Macedo, A. M., Teixeira, M.M.G., Sturm, N.R., 2012. The revised *Trypanosoma cruzi* subspecific nomenclature: Rationale, epidemiological relevance and research applications. *Infect. Genet. Evol.* 12 (2), 240–253. <https://doi.org/10.1016/j.meegid.2011.12.009>.